INRIA

INSTITUT NATIONAL DE RECHERCHE EN INFORMATIQUE ET EN AUTOMATIQUE

Some numerical aspects of the conservative PSM scheme in a 4D drift-kinetic code

Jean-Philippe Braeunig — Nicolas Crouseilles — Virginie Grandgirard — Guilaume Latu — Michel Mehrenberger — Eric Sonnendrücker

N° 7109

November 2009

Rapport de recherche

ISSN 0249-6399 ISRN INRIA/RR--7109--FR+ENG

INSTITUT NATIONAL DE RECHERCHE EN INFORMATIQUE ET EN AUTOMATIQUE
INRIA
centre de recherche NANCY - GRAND EST

Some numerical aspects of the conservative PSM scheme in a 4D drift-kinetic code

Jean-Philippe Braeunig*† ‡ , Nicolas Crouseilles * † , Virginie Grandgirard § , Guilaume Latu § ¶ * , Michel Mehrenberger† * , Eric Sonnendrücker† *

Thème : Modélisation, analyse numérique
Équipe-Projet CALVI

Rapport de recherche n° 7109 — November 2009 — 37 pages

Abstract: The purpose of this work is simulation of magnetised plasmas in the ITER project framework. In this context, Vlasov-Poisson like models are used to simulate core turbulence in the tokamak in a toroidal geometry. This leads to heavy simulation because a 6D dimensional problem has to be solved, 3D in space and 3D in velocity. The model is reduced to a 5D gyrokinetic model, taking advantage of the particular motion of particles due to the presence of a strong magnetic field. However, accurate schemes, parallel algorithms need to be designed to bear these simulations. This paper describes the numerical studies to improve robustness of the conservative PSM scheme in the context of its development in the GYSELA code. In this paper, we only consider the 4D drift-kinetic model which is the backbone of the 5D gyrokinetic models and relevant to build a robust and accurate numerical method.

Key-words: numerical simulation, conservative scheme, ITER, plasma turbulence

* INRIA Nancy-Grand Est, 615 rue du Jardin Botanique, 54600 Villers-lès-Nancy
† IRMA, Université de Strasbourg, 7 rue René-Descartes, 67084 Strasbourg Cedex
‡ CEA/DIF Bruyères-le-Châtel, 91297 Arpajon Cedex
§ CEA Cadarache, 13108 St Paul-lez-Durance Cedex
¶ LSIIT, Pole API, Boulevard Seb. Brant, 67400 Illkirch

Centre de recherche INRIA Nancy – Grand Est
LORIA, Technopôle de Nancy-Brabois, Campus scientifique,
615, rue du Jardin Botanique, BP 101, 54602 Villers-Lès-Nancy
Téléphone : +33 3 83 59 30 00 — Télécopie : +33 3 83 27 83 19

Some numerical aspects of the conservative PSM scheme in a 4D drift-kinetic code

Résumé : Ce travail concerne la simulation de plasmas magnétisés dans le cadre du projet ITER. Pour cette application, des modèles de type Vlasov-Poisson sont utilisés pour simuler la turbulence à coeur dans un tokamak, en géométrie toroidale. Ces études mènent à résoudre des problèmes dans un espace à 6 dimensions, 3D en espace 3D en vitesse, qui sont très lourds à simuler en terme de ressources informatiques. Le modèle est réduit à un modèle gyrocinétique 5D en exploitant les caractéristiques de ce plasma, dont le mouvement des particules est fortement influencé par la présence d'un champ magnétique intense. Cependant, il est nécessaire de mettre au point des schémas précis et des algorithmes parallèles pour mener ces simulations. Ce rapport décrit une étude numérique du schéma conservatif PSM dans le cadre de son intégration dans le code de calcul GYSELA. Dans ce travail, nous l'utilisons pour résoudre le modèle drift-kinetic 4D, qui est le squelette du modèle gyrocinétique 5D. Ce modèle 4D est suffisamment pertinent pour la conception d'une méthode numérique robuste et précise pour le modèle 5D.

Mots-clés : simulation numérique, schéma conservatif, ITER, turbulence plasma

1 Introduction

The ITER device is a tokamak designed to study controlled thermonuclear fusion. Roughly speaking, it is a toroidal vessel containing a magnetised plasma where fusion reactions occur. The plasma is kept out of the vessel walls by a magnetic field which lines have a specific helicoidal geometry. However, turbulence develops in the plasma and leads to thermal transport which decreases the confinement efficiency and thus needs a careful study. Plasma is constituted of ions and electrons, which motion is induced by the magnetic field. The characteristic mean free path is high, even compared with the vessel size, therefore a kinetic description of particles is required, see *Dimits* [4]. Then the full 6D Vlasov-Poisson should be used for both ions and electrons to properly describe the plasma evolution. However, the plasma flow in presence of a strong magnetic field has characteristics that allow some physical assumptions to reduce the model. First, the Larmor radius, i.e. the radius of the cyclotronic motion of particles around magnetic field lines, can be considered as small compared with the tokamak size and the gyration frequency very fast compared to the plasma frequency. Thus this motion can be averaged (gyro-average) becoming the so-called guiding center motion. As a consequence, 6D Vlasov-Poisson model is reduced to a 5D gyrokinetic model by averaging equations in such a way the 6D toroidal coordinate system $(r, \theta, \phi, v_r, v_\theta, v_\phi)$ becomes a 5D coordinate system $(r, \theta, \phi, v_\parallel, \mu)$, with $v_\parallel$ the parallel to the field lines component of the velocity and $\mu = m\ v_\perp^2/2B$ the adiabatic invariant which depends on the norm of the perpendicular to the field lines components of the velocity $v_\perp^2$, on the magnetic field magnitude B and on the particles mass m. Moreover, the magnetic field is assumed to be steady and the mass of electrons m_e is very small compared to the mass of ions m_i. Thus the cyclotron frequency $\omega_{i,e} = q_{i,e}\ B/m_{i,e}$ is assumed to be much faster for electrons than for ions $\omega_e >> \omega_i$. Therefore the electrons are assumed to be at equilibrium, i.e. the effect of the electrons cyclotronic motion is neglected and their distribution is then supposed to be constant in time. The 5D gyrokinetic model then reduces to a Vlasov like equation for ions guiding center motion:

$$\frac{\partial \bar{f}_\mu}{\partial t} + \frac{dX}{dt} \cdot \nabla_X \bar{f}_\mu + \frac{dv_\parallel}{dt} \partial_{v_\parallel} \bar{f}_\mu = 0 \tag{1}$$

where $\bar{f}_\mu(X, v_\parallel)$ is the ion distribution function with $X = (r, \theta, \phi)$, velocities dX/dt and $dv_\parallel/dt$ define the guiding center trajectories.
If $\nabla_{(X,v_\parallel)} \cdot (dX/dt, dv_\parallel/dt)^t = 0$, then the model is termed as conservative.
This equation for ions is coupled with a quasi-neutrality equation for the electric potential $\Phi(R)$ on real particles position, with $R = X - \rho_L$ (with ρ_L the Larmor radius) :

$$-\frac{1}{B\omega_i} \nabla_\perp \cdot (n_e \nabla_\perp \Phi) + \frac{e}{\kappa T_e} (\Phi - < \Phi >_{\theta,\phi}) = \int \bar{f}_\mu d\mu dv_\parallel - n_e \tag{2}$$

where n_e is an equilibrium electronic density, T_e the electronic temperature, e the electronic charge, κ the Boltzmann constant for electrons and ω_i the cyclotronic frequency for ions.

These equations are of a simple form, but they have to be solved very efficiently because of the 5D space and the large characteristic time scales con-

sidered. However, the adiabatic invariant μ acts as a parameter, thus it could easily be parallelised. Moreover, we can see that for each μ, we have to solve a 4D advection equation, as accurately as possible but also taking special care on mass and energy conservation, especially in this context of large characteristic time scales. The maximum principle that exists at the continuous level for the Vlasov equation should also be carefully studied at discrete level because there is no physical dissipation process in this model that might dissipate over/undershoots of the scheme. Those studies will be achieved first on a relevant reduced model, the 4D drift-kinetic model which corresponds to (1) with $\mu = 0$. This work follows those of *Grandgirard et al* in the GYSELA code, see [6] and [7]. The geometrical assumptions of this model for ion plasma turbulence are a cylindrical geometry with coordinates $(r, \theta, z, v_\parallel)$ and a constant magnetic field $B = B_z\ e_z$, where e_z is the unit vector in z direction. In this collisionless plasma, the trajectories are governed by the guiding center (GC) trajectories:

$$\frac{dr}{dt} = v_{GC_r};\ r\frac{d\theta}{dt} = v_{GC_\theta};\ \frac{dz}{dt} = v_\parallel;\ \frac{dv_\parallel}{dt} = \frac{q_i}{m_i}E_z \tag{3}$$

with $v_{GC} = (E \times B)/B^2$ and $E = -\nabla\Phi$ with Φ the electric potential.
The Vlasov equation governing this system, with the ion distribution function $f(r, \theta, z, v_\parallel, t)$, is the following:

$$\partial_t f + v_{GC_r}\partial_r f + v_{GC_\theta}\partial_\theta f + v_\parallel \partial_z f + \frac{q_i}{m_i}E_z\partial_{v_\parallel} f = 0. \tag{4}$$

This equation is coupled with a quasi-neutrality equation for the electric potential $\Phi(r, \theta, z)$ that reads the same as for the 5D gyrokinetic model (2) with $\mu = 0$. Let us notice that the 4D velocity field $a = (v_{GC_r}, v_{GC_\theta}, v_\parallel, q/m_i\ E_z)^t$ is divergence free:

$$\nabla \cdot a = \frac{1}{r}\partial_r(r\ v_{GC_r}) + \frac{1}{r}\partial_\theta(v_{GC_\theta}) + \partial_z v_\parallel + \partial_{v_\parallel}(q_i/m_i\ E_z) = 0 \tag{5}$$

because of variable independence $\partial_{v_\parallel} E_z = \partial_{v_\parallel}(\partial_z\Phi(r, \theta, z)) = 0$ and $\partial_z v_\parallel = 0$. Moreover we have $v_{GC} = (E \times B)/B^2$, with $E = -\nabla\Phi$ and $B = B_z\ e_z$, thus:

$$v_{GC_r} = \frac{1}{B_z}\left(-\frac{1}{r}\partial_\theta\Phi\right) \quad \text{and} \quad v_{GC_\theta} = \frac{1}{B_z}\left(\partial_r\Phi\right) \tag{6}$$

and

$$\nabla_{r\theta} \cdot a = \frac{1}{r}\partial_r(r\ v_{GC_r}) + \frac{1}{r}\partial_\theta(v_{GC_\theta}) = \frac{1}{r\ B_z}\left(\partial_r\left(r\ (-1/r)\partial_\theta\Phi\right) + \partial_\theta\left(\partial_r\Phi\right)\right) = 0. \tag{7}$$

Therefore, one can write an equivalent conservative equation to the preceding Vlasov equation (4):

$$\partial_t f + \partial_r(v_{GC_r}\ f) + \partial_\theta(v_{GC_\theta}\ f) + \partial_z(v_\parallel\ f) + \partial_{v_\parallel}\left(\frac{q_i}{m_i}E_z\ f\right) = 0. \tag{8}$$

This conservative system will be discretized using a conservative semi-Lagrangian scheme, the Parabolic Spline Method (PSM, see *Zerroukat et al* [13] and [14]) scheme. It is a fourth order scheme which is equivalent for linear advections

to the Backward Semi-Lagrangian scheme (BSL, see *Cheng-Knorr* [3] and *Sonnendrücker et al* [11]), but in a conservative form. This conservative scheme based on the conservative form of the Vlasov equation properly allows a directional splitting. This allows to handle easily any curvilinear coordinates system on structured grids. Therefore the Vlasov equation will be solved by using D (dimensions of space) 1D conservative steps, discretized by using the $1D$ PSM scheme.

In this paper, the BSL and PSM schemes will be detailed with an emphasis on their similarities and differences. We will see that one of the big difference is about the maximum principle. Although the BSL scheme does not strictly satisfy it, it is a real care for PSM scheme discretization in the context of a directional splitting. Indeed, the most difficult point is that each $1D$ step has no maximum principle, it is only the solution after all D directional steps, the solution of the Vlasov equation, that should satisfy a maximum principle. It is then a difficult task to design a slope/flux limiting procedure to satisfy the maximum principle for the discrete solution. We propose a flux limiter, called "entropic flux limiter", based on Finite Volumes schemes techniques that does not ensure a maximum principle, but only cuts off the anti-dissipative behaviour of the PSM scheme. This flux limiter makes the formally fourth order in the phase space variables PSM scheme degenerate into a second order scheme when the scheme has an anti-dissipative behaviour. Moreover, the maximum principle strongly depends on volumes conservation in the phase space during one time step, i.e. all D directional steps. This is equivalent to try to impose that the total divergence of the velocity field is null at the discrete level. Some rules are given to satisfy this constraint as well as a proposition to try to satisfy it.

The outline of this paper is the following : in section 2 will be recalled some important properties of Vlasov equations. Then BSL and PSM schemes will be described and compared, according to properties of the discrete solutions. In section 3, some criterions will be studied to improve the respect of Vlasov equations maximum principle when using the PSM scheme. In the same way, a flux limiter will be proposed to improve simulations robustness. In section 4, practical aspects of the PSM scheme use will be described in the context of the 4D drift-kinetic model and at last we will comment on numerical results.

2 Semi-Lagrangian schemes for Vlasov equation

2.1 Basics of the Vlasov equation

Let us consider an advection equation of a positive scalar function $f(x,t)$ with an arbitrary velocity field, but with a divergence free property:

$$\begin{cases} \partial_t f + a \cdot \nabla_x(f) = 0 \\ \nabla \cdot a = 0 \\ f(x,t) \geq 0 \end{cases} \tag{9}$$

with position $x \in \mathbb{R}^D$ and $a(x,t) \in \mathbb{R}^D$ the advection velocity field.
Since $\nabla \cdot a = 0$, we can use an equivalent conservative formulation of the Vlasov equation:

$$\partial_t f + \nabla_x \cdot (a\ f) = 0.$$

The solutions satisfy the maximum principle:

$$0 \leq f(x,t) \leq \max_x(f(x,t_0)) \tag{10}$$

for any initial time $t_0 < t$.
Moreover, for a closed physical domain Ω (for instance bounded with periodic boundary conditions), any L^p norm of the distribution function is conserved:

$$\frac{d}{dt}\left(\int_\Omega f^p(x,t)dx\right) = 0. \tag{11}$$

For more details, see *Sonnendrücker* Lecture Notes [12].

2.2 Basics of Lagrangian motion

Let us consider a conservative advection equation with an arbitrary velocity field:

$$\partial_t f + \nabla_x \cdot (a\ f) = 0, \tag{12}$$

with $f(x,t)$ a scalar function, position $x \in \mathbb{R}^D$ and $a(x,t) \in \mathbb{R}^D$.
One obvious property of this conservation law (Reynolds transport theorem) is to conserve the mass

$$d_t m = d_t \int_{Vol(t)} f(x,t) d\Omega = 0$$

in a Lagrangian volume $Vol(t)$.
Let us introduce the convective derivative $d_t(.) = \partial_t(.) + a \cdot \nabla_x(.)$, thus (12) becomes:

$$d_t f + f\ \nabla_x \cdot a = 0. \tag{13}$$

Considering a Lagrangian motion of an infinitely small volume $Vol(t)$, we have $d_t m = d_t(f\ Vol) = 0$. Thus we obtain:

$$\frac{d_t Vol}{Vol} = \nabla_x \cdot a. \tag{14}$$

We thus have a relation between the volume evolution and the velocity field a. In particular:

$$\frac{d_t Vol}{Vol} = 0 \Leftrightarrow \nabla_x \cdot a = 0. \tag{15}$$

2.3 Differences and similarities between BSL and PSM

2.3.1 Backward semi-Lagrangian (BSL)

Let us consider a Vlasov equation of the form:

$$\partial_t f + a \cdot \nabla_x f = 0, \tag{16}$$

with $f(x,t)$ a scalar function, position $x \in \mathbb{R}^D$ and $a(x,t) \in \mathbb{R}^D$ the advection field.
In the BSL scheme, see *Sonnendrücker et al* [11], the invariance property of function f along characteristic curves is used to obtain values f^{n+1} at time t^{n+1} from the values f^n at t^n:

$$f^{n+1}\left(X(x^{n+1},t^{n+1})\right) = f^n\left(X(x^{n+1},t^n)\right), \tag{17}$$

with x the Eulerian coordinates and the characteristic curves X defined as $\dfrac{dX(x,t)}{dt} = a(x,t)$ with the initial position $x = X(x,t^n)$ at t^n.
Let us locate the discrete function values f_i^n at mesh nodes. From a numerical point of view, we solve the following nonlinear system which is a second order approximation of $d_t X(t) = a(x,t)$:

$$\begin{array}{rcl} \dfrac{X(x_i^{n+1},t^{n+1}) - X(x_i^{n+1},t^n)}{\Delta t} & = & a\left(X_i^{n+1/2}, t^{n+1/2}\right), \\ X_i^{n+1/2} & = & \dfrac{X(x_i^{n+1},t^{n+1}) + X(x_i^{n+1},t^n)}{2}, \\ f^{n+1}\left(X(x_i^{n+1},t^{n+1})\right) & = & f^n\left(X(x_i^{n+1},t^n)\right), \end{array} \tag{18}$$

with x_i^{n+1} a node of the grid and $\Delta t = t^{n+1} - t^n$.
The scheme consists of two steps:

- To obtain the function value f_i^{n+1} at time t^{n+1} at a mesh node i which location is settled as $x_i^{n+1} = X(x_i^{n+1},t^{n+1})$, one has to follow backward the characteristic curve to find the "foot" $x_i^n = X(x_i^{n+1},t^n)$.
- Reconstruction (cubic spline) of function $f(x,t^n)$ on the domain to obtain its value at x_i^n, which is not a mesh node in general. Thus we have $f^{n+1}\left(x_i^{n+1}\right) = f^n\left(x_i^n\right)$.

2.3.2 Properties of the BSL scheme

This scheme is formally fourth order in space. It is second order in time using for instance a Leap-Frog, Predictor-Corrector or Runge-Kutta time integration.

Mass is not exactly conserved by this scheme, because it has no conservative form.

An approximated maximum principle is satisfied. Let us consider $f_h^n(x)$ the cubic spline interpolation of the distribution function $f^n(x) = f(x,t^n)$ at time t^n. Whatever the integration scheme to find the foot on the characteristic curve $X(x,t^n)$, we have for any x:

$$f^{n+1}\left(X(x,t^{n+1})\right) = f_h^n\left(X(x,t^n)\right)$$

with $f^n(x)$ the distribution function at time t^n.
It then naturally appears a "discrete" maximum principle:

$$\min_x(f_h^n(x,t^n)) \leq f^{n+1}(x) \leq \max_x(f_h^n(x,t^n)). \tag{19}$$

Of course, $\min_x(f_h^n(x,t^n)) \neq 0$ and $\max_x(f_h^n(x,t^n)) \neq \max_x(f^n(x,t^n))$, but if the cubic spline reconstruction is accurate enough, values should be close in such a way the stability of the scheme is granted. Moreover, if we can find a way to enforce a maximum principle of the cubic spline reconstruction, the BSL scheme maximum principle is granted.

Directional splitting is not allowed, because considering a $2D$ advection field (a_x, a_y):

$$\partial_t f + a_x\ \partial_x(f) + a_y\ \partial_y(f) = 0 \tag{20}$$

is not equivalent to compute the solution by directional splitting:

$$\begin{cases} \partial_t f + a_x\ \partial_x(f) = 0 \\ \partial_t f + a_y\ \partial_y(f) = 0. \end{cases} \tag{21}$$

Even if the velocity field $(a_x, a_y)^t$ is such that $\nabla \cdot (a_x, a_y)^t = 0$, each step of (21) is not conservative because $\partial_x a_x \neq 0$ and $\partial_y a_y \neq 0$ in general, see [8] to go further. A directional splitting is only allowed when using the conservative form (22), see section 2.3.3.

2.3.3 Parabolic Spline Method (PSM)

Let us consider a Vlasov equation in its conservative form:

$$\partial_t f + \nabla_x \cdot (a\ f) = 0, \tag{22}$$

with $f(x,t)$ a scalar function, position $x \in \mathbb{R}^D$ and $a(x,t) \in \mathbb{R}^D$ the advection field. Notice that with the hypothesis $\nabla_x \cdot (a) = 0$, conservative form (22) and non-conservative form (16) of the Vlasov equation are equivalent. In the PSM scheme, see *Zerroukat et al* [13] and [14], the conservation property of function f in a volume in Lagrangian motion is used to obtain values f^{n+1} at time t^{n+1}:

$$\int_{Vol^{n+1}} f(x,t^{n+1})d\Omega = \int_{Vol^n} f(x,t^n)d\Omega, \tag{23}$$

with the characteristic curves X defined as $\dfrac{dX(x,t)}{dt} = a(x,t)$ and $x = X(x,t^n)$ with t^n the initial time, and the volume $Vol^n = \{X(x^{n+1},t^n)$ such that $X(x^{n+1},t^{n+1}) \in Vol^{n+1}\}$ defined by the Lagrangian motion with the field $a(x,t)$.

The important point is that this conservative formalism properly allows a directional splitting without loosing the mass conservation when $\nabla_x \cdot (a) = 0$. Therefore, in a very convenient way, equation (22) may be solved with D successive 1D advections:

$$\frac{\partial f}{\partial t} + \partial_{x_k}(a_k\ f) = 0,\ k \in [1, D]. \tag{24}$$

From a numerical point of view, we then approximate a $1D$ equation for each direction k using the conservation property. Omitting subscript k, the PSM scheme writes in 1D as follows:

$$\int_{x_{i-1/2}^{n+1}}^{x_{i+1/2}^{n+1}} f(x,t^{n+1})dx = \int_{x_{i-1/2}^{n}}^{x_{i+1/2}^{n}} f(x,t^{n})dx, \tag{25}$$

with $x_{i+1/2}^{n+1} = X(x_{i+1/2}^{n+1},t^{n+1})$ settled as the 1D mesh nodes and $x_{i+1/2}^{n} = X(x_{i+1/2}^{n+1},t^{n})$, $Vol_i^n = [x_{i-1/2}^n, x_{i+1/2}^n]$ and $Vol_i^{n+1} = [x_{i-1/2}^{n+1}, x_{i+1/2}^{n+1}]$.
Let us define the average of f in cell i:

$$\overline{f}_i^{n+1} = \frac{1}{\Delta x}\int_{x_{i-1/2}^{n+1}}^{x_{i+1/2}^{n+1}} f(x,t^{n+1})dx, \tag{26}$$

with the uniform space step $\Delta x = x_{i-1/2}^{n+1} - x_{i+1/2}^{n+1}$ and the primitive function

$$F^n(z) = \int_{x_{1/2}}^{z} f(x,t^n)dx, \tag{27}$$

with $x_{1/2}$ an arbitrary reference point of the domain and for instance the first node of the grid $\{x_{i-1/2}\}_{i=1,N+1}$.

Therefore, one has to solve a nonlinear system, which is similar to the BSL one, to obtain a solution of equation (25) that simply writes:

$$\begin{array}{rcl} \dfrac{X(x_{i+1/2}^{n+1},t^{n+1}) - X(x_{i+1/2}^{n+1},t^{n})}{\Delta t} & = & a\left(X_{i+1/2}^{n+1/2}, t^{n+1/2}\right), \\ X_{i+1/2}^{n+1/2} & = & \dfrac{X(x_{i+1/2}^{n+1},t^{n+1}) + X(x_{i+1/2}^{n+1},t^{n})}{2}, \\ \overline{f}_i^{n+1}\Delta x & = & F^n(X(x_{i+1/2}^{n+1},t^n)) - F^n(X(x_{i-1/2}^{n+1},t^n)) \end{array} \tag{28}$$

with the time step $\Delta t = t^{n+1} - t^n$ and the uniform space step $\Delta x = x_{i+1/2}^{n+1} - x_{i-1/2}^{n+1}$.
The scheme is constituted with two steps:

- For a mesh node $i+1/2$ which location is settled as $x_{i+1/2}^{n+1} = X(x_{i+1/2}^{n+1},t^{n+1})$, one has to follow backward the characteristic curve to find the "foot" $x_{i+1/2}^{n} = X(x_{i+1/2}^{n+1},t^{n})$.

- Computation of the primitive function at mesh nodes $x_{i+1/2}^{n+1}$, what is a simple addition because for any $i \in [1,N]$:

$$F^n(x_{i+1/2}^{n+1}) - F^n(x_{1/2}) = \sum_{k=1}^{i} \overline{f}_k^n \Delta x,$$

  then interpolation (cubic spline) of the primitive function $F^n(z)$ on the domain with nodal values $F^n(x_{i+1/2}^{n+1})$ to obtain its value at $x_{i+1/2}^{n}$, which is not a mesh node in general. Thus we have
  $\overline{f}_i^{n+1}\Delta x = F^n(x_{i+1/2}^{n}) - F^n(x_{i-1/2}^{n})$.

The solution obtained using the PSM scheme with directional splitting is not the same that the one without splitting. The influence of this additional approximation is reduced by a Strang directional splitting. It consists in a second order time integration that improves the consistency of split operators to the unsplit one. Let us set for instance $A_x(\Delta t)$ the unsplit 2D PSM advection operator and $A_{x_k}(\Delta t)$ the 1D PSM advection operator in direction k, with Δt the time step and $x = (x_1, x_2)$. The Strang directional splitting then reads:

$$f^{n+1} = A_{x_1}(\Delta t/2)\ A_{x_2}(\Delta t)\ A_{x_1}(\Delta t/2)\ f^n = A_x(\Delta t)\ f^n + o(\Delta t^2).$$

Notice that the advection field $a(x, t^n) \in \mathbb{R}^D$ is only computed at the beginning of the time step t^n, and is used at the same time t^n for each step of the directional splitting.

2.3.4 Properties of the PSM scheme

This scheme is formally fourth order in space and strictly equivalent to the BSL scheme for constant linear advection, see [2]. It is second order in time using for instance a Leap-Frog, Predictor-Corrector or Runge-Kutta time integration.

Mass is exactly conserved by this scheme, because for each step of the directional splitting, by integrating on the whole domain:

$$\begin{aligned} \int_{x_{1/2}^{n+1}}^{x_{N+1/2}^{n+1}} f(x, t^{n+1})dx &= \sum_{k=1}^{N} \overline{f}_k^{n+1} \Delta x = F^n(x_{N+1/2}^n) - F^n(x_{1/2}^n) \\ &= \int_{x_{1/2}^n}^{x_{N+1/2}^n} f(x, t^n)dx. \end{aligned} \tag{29}$$

For each $1D$ step k of the directional splitting, no maximum principle does exist, even at the approximate sense shown for the BSL scheme in section 2.3.2, because in general $\partial_{x_k} a \neq 0$ even if the multi-dimensional field is divergence free $\nabla \cdot a = 0$. The maximum principle for non constant advections only exists considering all steps of the dimensional splitting. The PSM scheme will be studied in this context in section 3.1.

2.4 Finite volumes form of the PSM scheme

Let us consider the $1D$ conservative advection equation of the form:

$$\frac{\partial f}{\partial t} + \partial_x(a\ f) = 0, \tag{30}$$

with $f(x, t)$ a scalar function, position $x \in \mathbb{R}$ and $a(x, t) \in \mathbb{R}$ the advection field.

We recall that $X(x_{i+1/2}^{n+1}, t^{n+1}) = x_{i+1/2}$ is the position of the mesh node $i + 1/2$. Let us set the notation $X(x_{i+1/2}^{n+1}, t^n) = x_{i+1/2}^*$ for the "foot" position on the characteristic curve.
Let us rewrite the PSM scheme:

$$d_{i+1/2} = x_{i+1/2} - x_{i+1/2}^* = \Delta t\ a\left((x_{i+1/2} + x_{i+1/2}^*)/2, t^{n+1/2}\right)$$

$$\overline{f}_i^{n+1}\Delta x = F^n(x^*_{i+1/2}) - F^n(x^*_{i-1/2})$$

with $d_{i+1/2}$ the displacement of the node $x_{i+1/2}$.

Let us write the PSM scheme in the classical conservative form by making appear explicitly in $1D$ the fluxes at cell faces $i+1/2$ and $i-1/2$. By introducing the primitive values at cell faces $F^n(x_{i\pm\ 1/2})$:

$$\overline{f}_i^{n+1}\Delta x = \Big(F^n(x^*_{i+1/2}) - F^n(x_{i+1/2})\Big) - \Big(F^n(x^*_{i-1/2}) - F^n(x_{i-1/2})\Big) + \overline{f}_i^n\Delta x$$

with

$$\overline{f}_i^n\Delta x = F^n(x_{i+1/2}) - F^n(x_{i-1/2}).$$

It yields

$$\frac{\overline{f}_i^{n+1} - \overline{f}_i^n}{\Delta t} + \frac{F^n(x_{i+1/2}) - F^n(x^*_{i+1/2})}{\Delta x\Delta t} - \frac{F^n(x_{i-1/2}) - F^n(x^*_{i-1/2})}{\Delta x\Delta t} = 0. \quad (31)$$

It clearly appear the PSM fluxes of f at cell faces $i \pm 1/2$:

$$\frac{\overline{f}_i^{n+1} - \overline{f}_i^n}{\Delta t} + \frac{\Phi^{PSM}_{i+1/2} - \Phi^{PSM}_{i-1/2}}{\Delta x} = 0 \quad (32)$$

with

$$\Phi^{PSM}_{i+1/2} = \frac{F^n(x_{i+1/2}) - F^n(x^*_{i+1/2})}{\Delta t}. \quad (33)$$

3 Stability conditions for the PSM scheme

3.1 Maximum principle condition for the PSM scheme

3.1.1 Set of conditions for the multi-dimensional unsplit PSM scheme

Although we use the PSM scheme with directional splitting as described in section 2.3.3, let us first consider the case of D dimensions of space without taking into account the directional splitting:

$$\partial_t f + \nabla\cdot(a\ f) = 0, \quad (34)$$

with $f(x,t)$ a scalar function, position $x \in \mathbb{R}^D$ and $a(x,t) \in \mathbb{R}^D$ the advection field.
Let us consider a cell i, where the solution is described at time t^{n+1} by its average in cell i:

$$\overline{f}_i^{n+1} = \frac{1}{Vol_i^{n+1}}\int_{Vol_i^{n+1}} f(x,t^{n+1})d\Omega,$$

with Vol_i^{n+1} settled as the cell i volume.
The unsplit form of the PSM scheme for cell i then writes:

$$\overline{f}_i^{n+1}Vol_i^{n+1} = \int_{Vol_i^{n+1}} f(x,t^{n+1})d\Omega = \int_{Vol_i^n} f(x,t^n)d\Omega, \quad (35)$$

with the characteristic curves X defined as $\dfrac{dX(x,t)}{dt} = a(x,t)$ and $x = X(x,t^n)$ with t^n the initial time, and the volume $Vol_i^n = \{X(x^{n+1},t^n)$ such that $X(x^{n+1},t^{n+1}) \in Vol_i^{n+1}\}$ defined by the Lagrangian motion with the field $a(x,t)$.
We thus obtain the following relation:

$$\overline{f}_i^{n+1} = \overline{f}_i^{n*} \frac{Vol_i^n}{Vol_i^{n+1}} \tag{36}$$

with

$$\overline{f}_i^{n*} = \frac{1}{Vol_i^n} \int_{Vol_i^n} f(x,t^n) d\Omega.$$

Here clearly appear two conditions, both difficult to satisfy especially in the context of a directional splitting, to have a maximum principle defined as follows:

$$\min_x(f(x,t^n)) \leq \overline{f}_i^{n+1} \leq \max_x(f(x,t^n)). \tag{37}$$

- Monotonicity of the cubic spline reconstruction:

$$\min_x(f(x,t^n)) \leq \overline{f}_i^{n*} \leq \max_x(f(x,t^n)). \tag{38}$$

- Conservation of volumes in the phase space at the discrete level:

$$Vol_i^n = Vol_i^{n+1}. \tag{39}$$

  This last condition is true at the continuous level while $\nabla \cdot a = 0$ and $d_t Vol = 0$ since we have $d_t Vol = Vol\ \nabla \cdot a = 0$, see equation (15) in section 2.2.

3.1.2 Set of conditions for the multi-dimensional split PSM scheme

When using a directional splitting for a D dimensions space, D equations $1D$ are written:

$$\frac{\partial f}{\partial t} + \partial_{x_k}(a_k\ f) = 0, \tag{40}$$

with directions $k \in [1,D]$ and the velocity field $a = (a_k)_{k=1..D}$.
For each direction k, the PSM scheme is written in $1D$. We would like to satisfy a maximum principle like (37) at best even with the directional splitting, i.e. the result $\overline{f}^{n+1}$ obtained after all steps should satisfy the same property and the volume in the phase space should be conserved $Vol_i^n = Vol_i^{n+1}$.
Notice that for each $1D$ direction k, the mean values $\overline{f}_i^n$ are positioned at the cell center (x_i^k) and primitive function values are computed at cell faces center $(x_{i+1/2}^k)$. Following backward the characteristic curves, we obtain:

$$x_{i+1/2}^k - x_{i+1/2}^{k*} = \Delta t\ a_k \left((x_{i+1/2}^k + x_{i+1/2}^{k*})/2, t^{n+1/2} \right)$$

$$\overline{f}_i^{n+1} \Delta x = F^n(x_{i+1/2}^{k*}) - F^n(x_{i-1/2}^{k*})$$

with $x_{i+1/2}^{k*}$ "foot" of $x_{i+1/2}^k$ on the characteristic curve in direction k.

3.1.3 Monotonicity of the cubic spline reconstruction

Condition on the function reconstruction and integration (38) is very difficult to ensure for two reasons:

- First because for each $1D$ step of the directional splitting, there is no maximum principle for non constant advections even at continuous level. The monotonicity of the reconstruction might only exist considering the whole time step including all $1D$ advections.
- Second because it is the primitive $F^n(x)$ of the distribution function $f^n(x)$ that is reconstructed by cubic spline and not the function itself.

Therefore, we consider that the cubic spline reconstruction is accurate enough to provide a reliable discrete value of $\overline{f}_i^{n*}$.

3.1.4 Conservation of volumes in the phase space

The other condition to have a maximum principle for the PSM scheme is to satisfy the multi-dimensional condition (39), i.e. $Vol^n = Vol^{n+1}$. Equation (15) showed at continuous level that the volume evolution is constant in the phase space if the advection field is divergence free. Therefore we will study the PSM scheme to find a divergence free condition that should be satisfied at the discrete level $\nabla^h \cdot a = 0$ in such a way $Vol^n = Vol^{n+1}$, in the same way $\nabla \cdot a = 0$ at the continuous level. Such a discrete condition obviously involves all steps of the directional splitting. The directional splitting has an influence on the effective advection field used by the scheme and thus has an influence on the discrete operator $\nabla^h \cdot a = 0$. We do not want to make this condition depend on the time integration scheme, because a is the the field imposed by the model that the scheme must respect at best and the condition might be used for different time integration schemes. Therefore, we choose to study the scheme at first order in time and space, and without a directional splitting, in such a way second or further order terms in time do not interact with the research of an independent condition $\nabla^h \cdot a = 0$. To make appear the total evolution of volumes between t^n and t^{n+1}, we will use the finite volumes form of the PSM scheme in $2D$ given in 2.4, for the cartesian and polar coordinate systems.

Let us begin with the $2D$ cartesian case. Let us consider two directions (x, y), with constant space steps Δx, Δy and the cell volume is $Vol_{i,j} = \Delta x \Delta y$ centred on (x_i, y_j). Let us set a velocity field $(a_x(x, y), a_y(x, y))$ such that $\nabla_{x,y} \cdot a = 0$. Let us write the conservative advection equation in cartesian coordinates:

$$\partial_t f + \partial_x(a_x\ f) + \partial_y(a_y\ f) = 0. \tag{41}$$

The first order PSM scheme in the finite volumes form reads:

$$\frac{\overline{f}_{i,j}^{n+1} - \overline{f}_{i,j}^{n}}{\Delta t} + \frac{\Phi_{i+1/2,j}^{PSM,x} - \Phi_{i-1/2,j}^{PSM,x}}{\Delta x} + \frac{\Phi_{i,j+1/2}^{PSM,y} - \Phi_{i,j-1/2}^{PSM,y}}{\Delta y} = 0 \tag{42}$$

with $\Phi^{PSM,y}_{i,j\pm1/2}$ and $\Phi^{PSM,x}_{i\pm1/2,j}$ positioned at cell faces center and

$$\begin{aligned}\Phi^{PSM,x}_{i+1/2,j}\ \Delta t &= F^n(x_{i+1/2},y_j) - F^n(x^*_{i+1/2},y_j) = \int_{x^*_{i+1/2}}^{x_{i+1/2}} f(x,y_j,t^n)dx \\ \Phi^{PSM,y}_{i,j+1/2}\ \Delta t &= F^n(x_i,y_{j+1/2}) - F^n(x_i,y^*_{j+1/2}) = \int_{y^*_{j+1/2}}^{y_{j+1/2}} f(x_i,y,t^n)dy\end{aligned} \tag{43}$$

with

$$F^n(z,y_j) = \int_{x_{1/2}}^{z} f(x,y_j,t^n)dx$$

$$F^n(x_i,z) = \int_{y_{1/2}}^{z} f(x_i,y,t^n)dy$$

and values in cell i at time t^n and t^{n+1}
$\overline{f}^n_{i,j}\ \Delta x\Delta y = \int_{Vol_{i,j}} f(x,y,t^n)dxdy,$
$\overline{f}^{n+1}_{i,j}\ \Delta x\Delta y = \int_{Vol_{i,j}} f(x,y,t^{n+1})dxdy$
with $x_{i\pm1/2}$ the node position and $x^*_{i\pm1/2}$ the "foot" of this node (obvious same form in y direction) obtained with an first order scheme:

$$x_{i\pm1/2} - x^*_{i\pm1/2} = \Delta t\ a(x_{i\pm1/2},y_j,t^n).$$

Using preceding integral forms of each term, equation (42) becomes:

$$\begin{aligned}&\frac{1}{\Delta x\Delta y}\int_{\Delta x\Delta y} f(x,y,t^{n+1})dxdy - \frac{1}{\Delta x\Delta y}\int_{\Delta x\Delta y} f(x,y,t^n)dxdy + \\ &\left(\int_{x^*_{i+1/2}}^{x_{i+1/2}} f(x,y_j,t^n)dx - \int_{x^*_{i-1/2}}^{x_{i-1/2}} f(x,y_j,t^n)dx\right)/\Delta x + \\ &\left(\int_{y^*_{j+1/2}}^{y_{j+1/2}} f(x_i,y,t^n)dy - \int_{y^*_{j-1/2}}^{y_{j-1/2}} f(x_i,y,t^n)dy\right)/\Delta y = 0.\end{aligned} \tag{44}$$

Let us recall that for a line i (respectively j) of the mesh, the cell average $\overline{f}_{i,j}$ of the distribution function leads to constant values in perpendicular directions to x (respectively y) in the cell $Vol_{i,j}$, thus:

$$\int_{x^*_{i+1/2}}^{x_{i+1/2}} f(x,y_j,t^n)dx = \int_{x^*_{i+1/2}}^{x_{i+1/2}} f(x,y,t^n)dx$$

$$\int_{y^*_{j+1/2}}^{y_{j+1/2}} f(x_i,y,t^n)dy = \int_{y^*_{j+1/2}}^{y_{j+1/2}} f(x,y,t^n)dy.$$

Let us introduce volume displacements:

$$\delta Vol^x_{i\pm1/2} = \Delta y\ (x_{i\pm1/2} - x^*_{i\pm1/2}) \ \text{ and } \ \delta Vol^y_{j\pm1/2} = \Delta x\ (y_{j\pm1/2} - y^*_{j\pm1/2}).$$

From (44), we obtain:

$$\int_{Vol_{i,j}} f(x,y,t^{n+1})dxdy = \int_{Vol^n_{i,j}} f(x,y,t^n)dxdy \tag{45}$$

with

$$Vol^n_{i,j} = Vol_{i,j} - \delta Vol^x_{i+1/2} + \delta Vol^x_{i-1/2} - \delta Vol^y_{j+1/2} + \delta Vol^y_{j-1/2}.$$

We here recover a discrete mass conservation formulation. To obtain a maximum principle, we should have $Vol_{i,j} = Vol^n_{i,j}$, therefore:

$$\delta Vol^x_{i+1/2} - \delta Vol^x_{i-1/2} + \delta Vol^y_{j+1/2} - \delta Vol^y_{j-1/2} = 0.$$

Using δVol^k definitions, we obtain a discrete divergence formulation $\nabla^h \cdot a = 0$:

$$\frac{a_x(x_{i+1/2}, y_j) - a_x(x_{i-1/2}, y_j)}{\Delta x} + \frac{a_y(x_i, y_{j+1/2}) - a_y(x_i, y_{j-1/2})}{\Delta y} = 0. \quad (46)$$

Let us treat the $2D$ polar coordinates. Let us consider radial r and orthoradial θ directions, with constant space steps Δr, $\Delta\theta$ and the volume of the cells is exactly $Vol_{i,j} = r_i \Delta r \Delta\theta$. Let us set a velocity field $(a_r(r,\theta), r\ a_\theta(r,\theta))$ such that:

$$\nabla_{r,\theta} \cdot a = \frac{1}{r}\partial_r(r\ a_r) + \frac{1}{r}\partial_\theta(r\ a_\theta) = 0.$$

Let us write the conservative advection equation in polar coordinates:

$$\partial_t f + \frac{1}{r}\partial_r(r\ a_r\ f) + \frac{1}{r}\partial_\theta(r\ a_\theta\ f) = 0. \quad (47)$$

With the change of variable $g = r\ f$, it comes:

$$\partial_t g + \frac{\partial_r(a_r\ g)}{\partial r} + \frac{\partial_r(a_\theta\ g)}{\partial \theta} = 0. \quad (48)$$

The PSM scheme without directional splitting in the finite volumes form reads:

$$\frac{\overline{g}^{n+1}_{i,j} - \overline{g}^n_{i,j}}{\Delta t} + \frac{\Phi^{PSM,r}_{i+1/2,j} - \Phi^{PSM,r}_{i-1/2,j}}{\Delta r} + \frac{\Phi^{PSM,\theta}_{i,j+1/2} - \Phi^{PSM,\theta}_{i,j-1/2}}{\Delta \theta} = 0 \quad (49)$$

with $\Phi^{PSM,\theta}_{i,j\pm1/2}$ and $\Phi^{PSM,r}_{i\pm1/2,j}$ positioned at center of cell faces.
The cell averaged values of $\overline{g}$ used in the scheme are:

$$\overline{g}_{i,j} = r_i \overline{f}_{i,j} = r_i \frac{1}{Vol_{i,j}} \int_{Vol_{i,j}} f(r,\theta,t)\ r dr d\theta. \quad (50)$$

Using the integral form of each term and following the cartesian case (44):

$$\begin{gathered} r_i(\overline{f}^{n+1}_{i,j} - \overline{f}^n_{i,j}) + \\ \left(\int_{r^*_{i+1/2}}^{r_{i+1/2}} g(r,\theta_i,t^n)dr - \int_{r^*_{i-1/2}}^{r_{i-1/2}} g(r,\theta_i,t^n)dr \right)/\Delta r + \\ \left(\int_{\theta^*_{j+1/2}}^{\theta_{j+1/2}} g(r_i,\theta,t^n)d\theta - \int_{\theta^*_{j-1/2}}^{\theta_{j-1/2}} g(r_i,\theta,t^n)d\theta \right)/\Delta\theta = 0. \end{gathered} \quad (51)$$

Let us recall that for a line i (respectively j) of the mesh, the cell average $\overline{f}_{i,j}$ of the distribution function leads to constant values in perpendicular directions to r (respectively θ) in the cell $Vol_{i,j}$, thus:

$$\int_{r^*_{i+1/2}}^{r_{i+1/2}} g(r,\theta_j,t^n)dr = \int_{r^*_{i+1/2}}^{r_{i+1/2}} g(r,\theta,t^n)dr = \overline{r}_{i+1/2} \int_{r^*_{i+1/2}}^{r_{i+1/2}} f(r,\theta,t^n)dr$$

$$\int_{\theta^*_{j+1/2}}^{\theta_{j+1/2}} g(r_i,\theta,t^n)d\theta = r_i \int_{\theta^*_{j+1/2}}^{\theta_{j+1/2}} f(r,\theta,t^n)d\theta$$

with $\overline{r}_{i+1/2} \in [r^*_{i+1/2}, r_{i+1/2}]$ defined implicitely.
Let us introduce volume displacements:

$\delta Vol^r_{i\pm1/2} = \overline{r}_{i\pm1/2}\ \Delta\theta\ (r_{i\pm1/2} - r^*_{i\pm1/2})$ and $\delta Vol^\theta_{j\pm1/2} = r_i\ \Delta r\ (\theta_{j\pm1/2} - \theta^*_{j\pm1/2})$.

Therefore we obtain:

$$\int_{Vol_{i,j}} f(r,\theta,t^{n+1})\ r\ drd\theta = \int_{Vol^n_{i,j}} f(r,\theta,t^n)\ r\ drd\theta \tag{52}$$

with

$$Vol^n_{i,j} = Vol_{i,j} - \delta Vol^r_{i+1/2} + \delta Vol^r_{i-1/2} - \delta Vol^\theta_{j+1/2} + \delta Vol^\theta_{j-1/2}.$$

We here recover a discrete mass conservation formulation. To obtain a maximum principle, we should have $Vol_{i,j} = Vol^n_{i,j}$, therefore:

$$\delta Vol^r_{i+1/2} - \delta Vol^r_{i-1/2} + \delta Vol^\theta_{j+1/2} - \delta Vol^\theta_{j-1/2} = 0.$$

Using δVol^k definitions, we obtain:

$$\begin{array}{l} \dfrac{1}{r_i}\dfrac{\overline{r}_{i+1/2}a_r(r_{i+1/2},\theta_j) - \overline{r}_{i-1/2}a_r(r_{i-1/2},\theta_j)}{\Delta r} + \\ \dfrac{1}{r_i}\dfrac{r_i a_\theta(r_i,\theta_{j+1/2}) - r_i a_\theta(r_i,\theta_{j-1/2})}{\Delta\theta} = 0. \end{array} \tag{53}$$

Using the following first order approximation, to get rid of the dependency of the "foot" $r^*_{i+1/2}$ calculation depending on the integration scheme:

$$r_{i+1/2} \approx \overline{r}_{i+1/2} = (r_{i+1/2} + r^*_{i+1/2})/2,$$

we thus obtain a discrete divergence formulation in polar coordinates $\nabla^h \cdot a = 0$ to be nullified:

$$\begin{array}{l} \dfrac{1}{r_i}\dfrac{r_{i+1/2}a_r(r_{i+1/2},\theta_j) - r_{i-1/2}a_r(r_{i-1/2},\theta_j)}{\Delta r} + \\ \dfrac{1}{r_i}\dfrac{r_i a_\theta(r_i,\theta_{j+1/2}) - r_i a_\theta(r_i,\theta_{j-1/2})}{\Delta\theta} = 0. \end{array} \tag{54}$$

As a conclusion, these first order discrete divergence formulations (46) and (54) are independent of the time integration method. It is a discrete consistent relation for the advection field of the form $\nabla^h \cdot a = 0$. It should be satisfied to get, with an first order error, the aimed conservation condition on volumes $Vol^n = Vol^{n+1}$ in the phase space, which is necessary to obtain a maximum principle for the PSM scheme. We experimentally notice that this condition is good enough and is actually necessary when using the fourth order PSM scheme with directional splitting as described in section 2.3.3. Notice that the advection field $a(x,t^n)$ is only computed at the beginning of the time step t^n, and is used at the same time t^n for each step of the directional splitting. Figures 2 and 1 compare the results of a 4D drift-kinetic benchmark (see section 4.4.2 for details) obtained with the PSM scheme 2.3.3 with an advection field computed: first in such a way the discrete divergence free condition (54) is satisfied and second with an advection field computed by cubic spline interpolation without satisfying this condition.

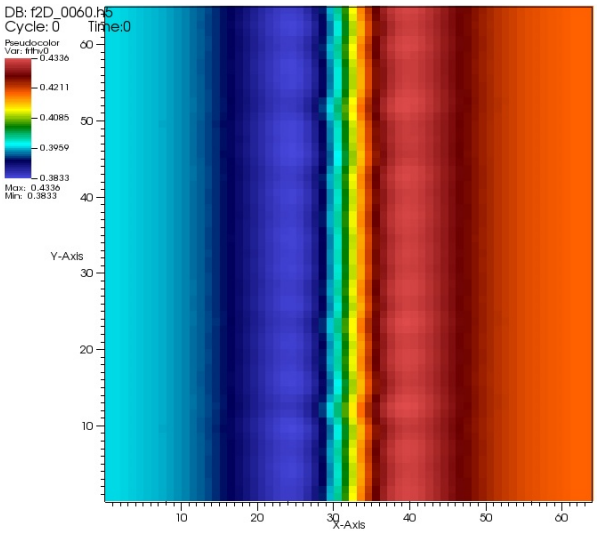

Figure 1: Result at time $t = 60$ with the advection field computed in a way (see section 4.4.2) that satisfy the discrete divergence condition (54).

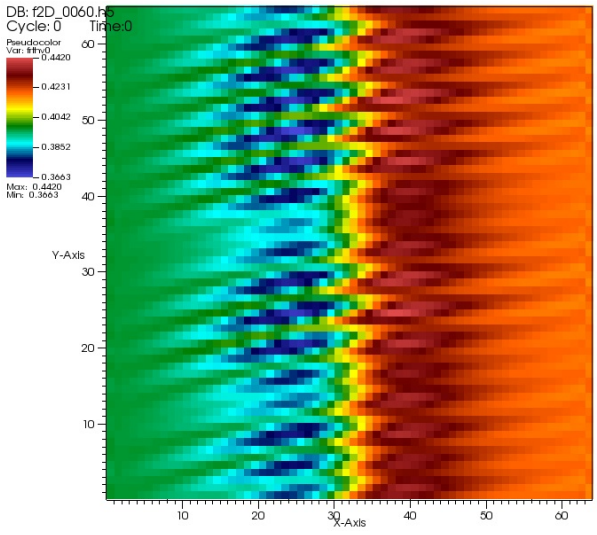

Figure 2: Result at time $t = 60$ with the advection field computed with cubic splines, which do not satisfy the discrete divergence condition (54).

Respecting condition (54) for the advection field not only leads to a better respect of the maximum principle, it is actually necessary to ensure the stability of the scheme. The result in figure 2 diverges from realistic physics.

3.2 A simple flux limiter for the PSM scheme

Some difficulties may arise when dealing with stiff profiles of the distribution function. Although the cubic spline reconstruction is accurate when dealing with smooth profiles, some spurious oscillations may appear when for instance filaments form in the flow. The idea here is to find a numerical limiter that prevents these oscillations.
A lot of methods of flux limiting exists in the context of finite volumes schemes, see *LeVeque* [9]. We want to adapt such strategies to the PSM scheme.

3.2.1 Second order equivalent equation of the PSM scheme

Let us perform a second order Taylor expansion of the PSM flux (33) of the variable displacement $d_{i+1/2} = x_{i+1/2} - x^*_{i+1/2}$ at the node position $x_{i+1/2}$:

$$\begin{aligned}\Phi^{PSM}_{i+1/2} &= \frac{F^n(x_{i+1/2}) - F^n(x_{i+1/2} - d_{i+1/2})}{\Delta t} \\ &= \frac{1}{\Delta t}\left(d_{i+1/2}\partial_x F^n(x_{i+1/2}) - \frac{(d_{i+1/2})^2}{2}\partial_{xx} F^n(x_{i+1/2}) + o(d_{i+1/2})^2 \right) \\ &= a^{n+1/2}_{i+1/2}\ f^n(x_{i+1/2}) - \frac{\Delta t \left(a^{n+1/2}_{i+1/2}\right)^2}{2}\partial_x f^n(x_{i+1/2}) + o(d_{i+1/2})^2\end{aligned} \tag{55}$$

with $d_{i+1/2} = \Delta t\ a^{n+1/2}_{i+1/2} = \Delta t\ a\left(X^{n+1/2}_{i+1/2}, t^{n+1/2}\right)$ and by definition $\partial_x F^n(x_{i+1/2}) = f^n(x_{i+1/2})$.
Of course, we see that this PSM flux Φ^{PSM} is an approximation of $\Phi = a\ f$, the flux at the continuous level. Moreover, we can see the second order equivalent equation that is also approximated by the scheme by injecting the second order approximation (55) in the scheme definition (32):

$$\begin{aligned}&\frac{\overline{f}^{n+1}_i - \overline{f}^n_i}{\Delta t} + \frac{a^{n+1/2}_{i+1/2} f^n(x_{i+1/2}) - a^{n+1/2}_{i-1/2} f^n(x_{i-1/2})}{\Delta x} = \\ &\frac{\Delta t}{2}\frac{\left(a^{n+1/2}_{i+1/2}\right)^2\ \partial_x f^n(x_{i+1/2}) - \left(a^{n+1/2}_{i-1/2}\right)^2 \partial_x f^n(x_{i-1/2})}{\Delta x} + o(d)^2\end{aligned} \tag{56}$$

The second order equivalent equation is then at the continuous level:

$$\frac{\partial f}{\partial t} + \partial_x(a\ f) = \frac{\Delta t}{2}\partial_x(a^2\ \partial_x f). \tag{57}$$

This equivalent second order equation is very nice, because the second order term appearing at the right hand side is a diffusion operator with an always positive diffusion coefficient $\Delta t\ a^2/2$. This indicates that the errors of the scheme should always lead to diffusion of the solution rather than dispersion, which is a good point for the robustness of the scheme.
However, the cubic spline reconstruction is not monotonic and may lead to errors when interpolating the primitive function $F^n(x)$. Therefore some spurious oscillations may appear when the derivatives $\partial_x f^n(x)$ are not well described through the primitive function reconstruction $F^n(x)$. Let us find a way to detect and correct these situations.

3.2.2 Measurement of the "upwinding"

Let us consider a basic "upwind" like scheme for the 1D conservative advection equation (34):

$$\frac{\partial f}{\partial t} + \partial_x(a\ f) = 0.$$

The scheme reads:

$$\begin{array}{l} \dfrac{f_i^{n+1} - f_i^n}{\Delta t} + \dfrac{\Phi_{i+1/2}^{UP} - \Phi_{i-1/2}^{UP}}{\Delta x} = 0 \\ \Phi_{i+1/2}^{UP} = a_{i+1/2}^{n+1/2} \left(\dfrac{f_{i+1}^n + f_i^n}{2} - sign(a_{i+1/2}^{n+1/2}) \dfrac{f_{i+1}^n - f_i^n}{2} \right) \end{array} \tag{58}$$

with $sign(a_{i+1/2}^{n+1/2})$ is the sign of the velocity $a_{i+1/2}^{n+1/2}$.
We can define as well a "centred" like scheme with the flux:

$$\Phi_{i+1/2}^{CEN} = a_{i+1/2}^{n+1/2} \left(\frac{f_{i+1}^n + f_i^n}{2} \right) \tag{59}$$

Let us finally consider an hybrid scheme "α-upwind" of both "upwind" and "centred" schemes:

$$\begin{array}{rl} \Phi_{i+1/2}^{\alpha UP} & = (1 - \alpha_{i+1/2}) \Phi_{i+1/2}^{CEN} + \alpha_{i+1/2}\ \Phi_{i+1/2}^{UP} \\ & = a_{i+1/2}^{n+1/2} \left(\dfrac{f_{i+1}^n + f_i^n}{2} - \alpha_{i+1/2}\ sign(a_{i+1/2}^{n+1/2}) \dfrac{f_{i+1}^n - f_i^n}{2} \right) \end{array} \tag{60}$$

with $0 \leq \alpha_{i+1/2} \leq 1$.
The parameter $\alpha_{i+1/2}$ is a way to evaluate the sign of the scheme diffusion coefficient in the sense of equation (56) because with the flux $\Phi_{i+1/2}^{\alpha UP}$, we have directly the form of the second order equivalent equation. Indeed, by replacing $\Phi_{i+1/2}^{\alpha UP}$ in (58):

$$\begin{array}{l} \dfrac{f_i^{n+1} - f_i^n}{\Delta t} + \dfrac{a_{i+1/2}^{n+1/2} f^n(x_{i+1/2}) - a_{i-1/2}^{n+1/2} f^n(x_{i-1/2})}{\Delta x} \\ = \dfrac{\alpha_{i+1/2} |a_{i+1/2}^{n+1/2}| (f_{i+1}^n - f_i^n) \ - \alpha_{i-1/2} |a_{i-1/2}^{n+1/2}| (f_i^n - f_{i-1}^n)}{\Delta x} \\ = \dfrac{\alpha_{i+1/2} |a_{i+1/2}^{n+1/2}| \Delta x\ \partial_x f^n(x_{i+1/2}) \ - \alpha_{i-1/2} |a_{i-1/2}^{n+1/2}| \Delta x\ \partial_x f^n(x_{i+1/2})}{\Delta x} + o(\Delta x) \\ = \partial_x \left(\alpha |a| \Delta x\ \partial_x f \right) + o(\Delta x) \end{array} \tag{61}$$

with $f^n(x_{i+1/2}) = (f^n(x_{i+1}) + f^n(x_i))/2 + o(\Delta x^2)$.

The Taylor expansion at last line of equation (61) shows that flux $\Phi_{i+1/2}^{\alpha UP}$ leads to a second order diffusion term with a diffusion coefficient $\alpha |a| \Delta x$. This scheme has then a dissipative behaviour if $\alpha_{i+1/2} > 0$. This is the key point for our flux limiter design : we want to modify the PSM flux to enforce a dissipative behaviour of the scheme when it is not the case, in the sense of $\alpha_{i+1/2} < 0$ for the $\Phi^{\alpha UP}$ flux.

3.2.3 Flux limiter definition

The flux limiting procedure we propose is the following:

After having computed $\Phi^{PSM}_{i+1/2}$, one can always find $\alpha_{i+1/2}$ for the flux $\Phi^{\alpha UP}_{i+1/2}$ in such a way:

$$\Phi^{PSM}_{i+1/2} = \Phi^{\alpha UP}_{i+1/2} \tag{62}$$

- if $\alpha_{i+1/2} \geq 0$ then we consider that the flux $\Phi^{PSM}_{i+1/2}$ is dissipative.
- if $\alpha_{i+1/2} < 0$ then we consider that the flux is not dissipative and we set $\alpha_{i+1/2} = 0$ by replacing $\Phi^{PSM}_{i+1/2} = \Phi^{CEN}_{i+1/2}$.

with fluxes expressions from equations (59) , (60) and (55):

$$\begin{aligned}
\Phi^{CEN}_{i+1/2} &= a^{n+1/2}_{i+1/2} f^n(x_{i+1/2}) \\
\Phi^{\alpha UP}_{i+1/2} &= a^{n+1/2}_{i+1/2} f^n(x_{i+1/2}) - \frac{\alpha_{i+1/2}\ |a^{n+1/2}_{i+1/2}|\ \Delta x}{2}\ \frac{f^n_{i+1} - f^n_i}{\Delta x} \\
\Phi^{PSM}_{i+1/2} &= a^{n+1/2}_{i+1/2}\ f^n(x_{i+1/2}) - \frac{\Delta t \left(a^{n+1/2}_{i+1/2}\right)^2}{2}\ \partial_x f^n(x_{i+1/2}) + o(d_{i+1/2})^2
\end{aligned} \tag{63}$$

with $f^n(x_{i+1/2}) = (f^n(x_{i+1}) + f^n(x_i))/2 + o(\Delta x)^2$.
This condition actually compares the decentred parts of fluxes.
If $\Phi^{PSM}_{i+1/2} = \Phi^{\alpha UP}_{i+1/2}$ then:

$$\Phi^{PSM}_{i+1/2} - \Phi^{CEN}_{i+1/2} = \Phi^{\alpha UP}_{i+1/2} - \Phi^{CEN}_{i+1/2} \tag{64}$$

which amounts to

$$-\frac{\Delta t \left(a^{n+1/2}_{i+1/2}\right)^2}{2} \partial_x f^n(x_{i+1/2}) + o(d_{i+1/2})^2 = -\alpha_{i+1/2}\ |a^{n+1/2}_{i+1/2}| \frac{f^n_{i+1} - f^n_i}{2}. \tag{65}$$

As a consequence, we set the following condition which imposes the decentred terms to have the same sign:

$$\alpha_{i+1/2}\ \left(f^n_{i+1} - f^n_i\right)\ \partial_x f^n(x_{i+1/2}) \geq 0 \tag{66}$$

We see that the condition $\alpha_{i+1/2} \geq 0$ is equivalent to watch if (and enforce if not) the effective derivative $\partial_x f^n(x_{i+1/2})$ computed by the scheme is of same sign than $\left(f^n_{i+1} - f^n_i\right)$.

We termed this limiter as "entropic flux limiter" because it leads to dissipate the numerical solution, what should make the physical entropy grow. In bad situations, this limiter makes the formally fourth order flux $\Phi^{PSM}_{i+1/2}$ degenerate into a second order flux, the centred flux $\Phi^{CEN}_{i+1/2}$.

3.2.4 Use of the entropic flux limiter for PSM

We have obtained the relation (66) as a consequence of the "entropic flux limiter". Considering relations (63) and (65), relation (66) is achieved limiting the PSM flux $\Phi^{PSM\ell}_{i+1/2}$ at second order with the following condition:
if $\left(\Phi^{CEN}_{i+1/2} - \Phi^{PSM}_{i+1/2}\right)\ \left(f^n_{i+1} - f^n_i\right) \geq 0$ then ok,
if $\left(\Phi^{CEN}_{i+1/2} - \Phi^{PSM}_{i+1/2}\right)\ \left(f^n_{i+1} - f^n_i\right) < 0$ then $\Phi^{PSM}_{i+1/2} = \Phi^{CEN}_{i+1/2}$.

Let us recall the relation between the PSM flux and the primitive of the distribution function:

$$\Delta t\ \Phi_{i+1/2}^{PSM} = F^n(x_{i+1/2}) - F^n(x_{i+1/2}^*). \tag{67}$$

Let us define a primitive function value F^{CEN} corresponding to the centred flux in the same formalism:

$$\Delta t\ \Phi_{i+1/2}^{CEN} = F^n(x_{i+1/2}) - F_{i+1/2}^{CEN}. \tag{68}$$

We then obtain the following conditions:
if $\left(F^n(x_{i+1/2}^*) - F_{i+1/2}^{CEN}\right)\ \left(f_{i+1}^n - f_i^n\right) \geq 0$ then ok,
if $\left(F^n(x_{i+1/2}^*) - F_{i+1/2}^{CEN}\right)\ \left(f_{i+1}^n - f_i^n\right) < 0$ then $F^n(x_{i+1/2}^*) = F_{i+1/2}^{CEN}$,

3.2.5 Entropic flux limiter algorithm for PSM

Let us now give an "entropic flux limitation" algorithm for the PSM scheme:

- Computation of displacements $d_{i+1/2}$ and "feet" $x_{i+1/2}^*$ on the characteristic curves:

$$d_{i+1/2} = x_{i+1/2} - x_{i+1/2}^* = \Delta t\ a\left((x_{i+1/2} + x_{i+1/2}^*)/2, t^{n+1/2}\right) \tag{69}$$

- Computation of the primitive values $F^n(x_{i+1/2}^*)$ by cubic spline reconstruction.
- Entropic flux limitation of values $F^n(x_{i+1/2}^*)$:
  if $\left(F^n(x_{i+1/2}^*) - F_{i+1/2}^{CEN}\right) \times \left(f_{i+1}^n - f_i^n\right) \geq 0$ then ok,
  if $\left(F^n(x_{i+1/2}^*) - F_{i+1/2}^{CEN}\right) \times \left(f_{i+1}^n - f_i^n\right) < 0$ then $F^n(x_{i+1/2}^*) = F_{i+1/2}^{CEN}$,
  with $F_{i+1/2}^{CEN} = F^n(x_{i+1/2}) - d_{i+1/2}\left(f^n(x_{i+1}) + f^n(x_i)\right)/2$
- Computation of the solution at time t^{n+1}:

$$\overline{f}_i^{n+1}\Delta x = F^n(x_{i+1/2}^*) - F^n(x_{i-1/2}^*).$$

Remark 1. *It is very convenient that this flux limiting procedure can be applied with a local algorithm. The computational cost of this flux limiting procedure is then very cheap. This is provided by the scheme conservativity that permits to work on fluxes at cell faces.*

4 Use of the PSM scheme in a 4D drift-kinetic code

4.1 Drift-kinetic model

This work follows those of *Grandgirard et al* in the GYSELA code, see [6] and [7]. The geometrical assumptions of this model for ion plasma turbulence are a cylindrical geometry with coordinates $(r, \theta, z, v_\parallel)$ and a constant magnetic field

$B = B_z\ e_z$, where e_z is the unit vector in z direction. In this collisionless plasma, the trajectories are governed by the guiding center (GC) trajectories:

$$\frac{dr}{dt} = v_{GC_r};\ r\frac{d\theta}{dt} = v_{GC_\theta};\ \frac{dz}{dt} = v_\parallel;\ \frac{dv_\parallel}{dt} = \frac{q_i}{m_i}E_z \tag{70}$$

with $v_{GC} = (E \times B)/B^2$ and $E = -\nabla\Phi$ with Φ the electric potential.
The Vlasov equation governing this system, where the ion distribution function is $f(r, \theta, z, v_\parallel, t)$, is the following:

$$\partial_t f + v_{GC_r}\partial_r f + v_{GC_\theta}\partial_\theta f + v_\parallel \partial_z f + \frac{q_i}{m_i}E_z\partial_{v_\parallel} f = 0. \tag{71}$$

This equation is coupled with a quasi-neutrality equation for the electric potential $\Phi(r, \theta, z)$ that reads:

$$-\nabla_\perp\Phi \cdot \left(\frac{n_0(r)}{B\ \Omega_0}\nabla\Phi\right) + \frac{e\ n_0(r)}{T_e(r)}(\Phi - < \Phi >_{\theta,z}) = n_i - n_0 \tag{72}$$

with $n_i = \displaystyle\int_{v_\parallel} f(r, \theta, z, v_\parallel)dv_\parallel$ and constant in time physical parameters n_0, Ω_0, T_e and e.
Let us notice that the 4D velocity field $a = (v_{GC_r}, v_{GC_\theta}, v_\parallel, q/m_i\ E_z)^t$ is divergence free:

$$\nabla \cdot a = \frac{1}{r}\partial_r(r\ v_{GC_r}) + \frac{1}{r}\partial_\theta(v_{GC_\theta}) + \partial_z v_\parallel + \partial_{v_\parallel}(q/m_i\ E_z) = 0 \tag{73}$$

because of variable independence $\partial_{v_\parallel}E_z = \partial_{v_\parallel}(\partial_z\Phi(r, \theta, z)) = 0$ and $\partial_z v_\parallel = 0$.
Moreover we have $v_{GC} = (E \times B)/B^2$, with $E = -\nabla\Phi$ and $B = B_z\ e_z$, thus:

$$v_{GC_r} = \frac{1}{B_z}\left(-\frac{1}{r}\partial_\theta\Phi\right) \quad \text{and} \quad v_{GC_\theta} = \frac{1}{B_z}\left(\partial_r\Phi\right) \tag{74}$$

and

$$\nabla_{r\theta} \cdot a = \frac{1}{r}\partial_r(r\ v_{GC_r}) + \frac{1}{r}\partial_\theta(v_{GC_\theta}) = \frac{1}{r\ B_z}\left(\partial_r\left(r\ (-1/r)\partial_\theta\Phi\right) + \partial_\theta\left(\partial_r\Phi\right)\right) = 0. \tag{75}$$

Therefore, one can write an equivalent conservative equation to the preceding Vlasov equation (71):

$$\partial_t f + \partial_r(v_{GC_r}\ f) + \partial_\theta(v_{GC_\theta}\ f) + \partial_z(v_\parallel\ f) + \partial_{v_\parallel}\left(\frac{q_i}{m_i}E_z\ f\right) = 0 \tag{76}$$

4.2 Computation of a divergence free velocity field at the discrete level

We have obtained a discrete form of the velocity field divergence to nullify (54) for sake of robustness of the scheme, namely to get nearby a maximum principle. We saw in (73) that $\nabla \cdot a = 0$ is satisfied equivalently if $\nabla_{r\theta} \cdot a = 0$ (75) is satisfied

and this is still true at the discrete level (independence of variables). Therefore, the velocity field should nullify the discrete polar divergence (54):

$$\frac{1}{r_i}\frac{r_{i+1/2}a_r(r_{i+1/2},\theta_j)-r_{i-1/2}a_r(r_{i-1/2},\theta_j)}{\Delta r}+ \frac{1}{r_i}\frac{r_i a_\theta(r_i,\theta_{j+1/2})-r_i a_\theta(r_i,\theta_{j-1/2})}{\Delta\theta}=0 \tag{77}$$

with

$$a_r = dr/dt = v_{GC_r} = \frac{-1}{r\ B_z}\partial_\theta\Phi$$

and

$$a_\theta = d\theta/dt = v_{GC_\theta}/r = \frac{1}{r\ B_z}\partial_r\Phi,$$

using definitions given in (74).

Proposition 2. *Let us define the electric potential at the nodes of the mesh $\Phi_{i+1/2,j+1/2}$, whatever the way it is computed.*
Let us set the following natural approximation for the velocity field:

$$\begin{aligned} a_r(r_{i+1/2},\theta_j) &= \frac{-1}{r_{i+1/2}\ B_z}\frac{\Phi_{i+1/2,j+1/2}-\Phi_{i+1/2,j-1/2}}{\Delta\theta} \\ a_\theta(r_i,\theta_{j+1/2}) &= \frac{1}{r_i\ B_z}\frac{\Phi_{i+1/2,j+1/2}-\Phi_{i-1/2,j+1/2}}{\Delta r}. \end{aligned} \tag{78}$$

With this approximated velocity field, the approximation of $\nabla_{r\theta}\cdot a = 0$ given in (77) is satisfied.

The proof is easy, we just have to put the velocity field (78) in (77), all terms annulate each others.

Remark 3. *Notice that electric potential Φ should be computed at nodes $(i+1/2, j+1/2)$ of the mesh to obtain velocities at the center of cell faces $(i\pm1/2, j)$ and $(i, j\pm1/2)$. It is well adapted to the PSM schemes, where the displacement should be calculated at cell faces, see section 2.3.3. Moreover, the advection field $a(x,t^n)\in\mathbb{R}^D$ is only computed at the beginning of the time step t^n, and is used at the same time t^n for each step of the directional splitting.*

4.3 Algorithm of the PSM sheme

At the beginning of the time step, the distribution function $f(x,v_\parallel,t^n)$ is known at time t^n, with $x=(r,\theta,z)$. The time step is $\Delta t = t^{n+1}-t^n$.

- The quasi-neutral equation is resolved using the distribution function $f(x,v_\parallel,t^n)$ to obtain the electric potential $\Phi^n(x)$ at time t^n.
- The advection field $a(x,t^n)=(a_r^n(x),a_\theta^n(x),a_z^n(x),a_{v_\parallel}^n(x))^t$ is computed with $\Phi^n(x)$ according to equation (73) and using formula (78) .
- PSM 1D advection of $f(x,v_\parallel,t^n)$ in direction $v_\parallel$ with velocity $a_{v_\parallel}^n$ and time step $\Delta t/2$ to obtain $f(x,v_\parallel,t^{v_\parallel/2})$.

- PSM 1D advection of $f(x, v_\parallel, t^{v_\parallel/2})$ in direction z with velocity a_z^n and time step $\Delta t/2$ to obtain $f(x, v_\parallel, t^{z/2})$.
- PSM 1D advection of $f(x, v_\parallel, t^{z/2})$ in direction θ with velocity a_θ^n and time step $\Delta t/2$ to obtain $f(x, v_\parallel, t^{\theta/2})$.
- PSM 1D advection of $f(x, v_\parallel, t^{\theta/2})$ in direction r with velocity a_r^n and time step Δt to obtain $f(x, v_\parallel, t^r)$.
- PSM 1D advection of $f(x, v_\parallel, t^r)$ in direction θ with velocity a_θ^n and time step $\Delta t/2$ to obtain $f(x, v_\parallel, t^\theta)$.
- PSM 1D advection of $f(x, v_\parallel, t^\theta)$ in direction z with velocity a_z^n and time step $\Delta t/2$ to obtain $f(x, v_\parallel, t^z)$.
- PSM 1D advection of $f(x, v_\parallel, t^z)$ in direction $v_\parallel$ with velocity $a_{v_\parallel}^n$ and time step $\Delta t/2$ to obtain $f(x, v_\parallel, t^{v_\parallel}) = f(x, v_\parallel, t^{n+1})$.

4.4 Numerical results

4.4.1 Test of the entropic flux limiter on constant 1D advections

We consider 1D advections on a periodic domain of length $L_x = 2$, with 120 cells, velocity $u_x = 0.05$, constant time step $\Delta t = 0.1$ and space step $\Delta x = 1.666\ 10^{-2}$. First two benchmarks, see figures 3 and 4, have initially sinusoidal shapes with $f \in [0, 2]$ with wave numbers 2 and 4. Third benchmark, see see figures 5, is initially a step function with $f(x) = 1$ for $x \in [0, 1]$ and with $f(x) = 0$ for $x \in [1, 2]$. The initial shapes travel 10 times the domain.
We compare results obtained with the PSM scheme (in red) and with the PSM scheme with entropic flux limiter (in green). Notice that results obtained using BSL and PSM schemes are identical, as it should be for linear advection.

4.4.2 Drift-kinetic 4D model, BSL-PSM-PSM with entropic limiter comparison

In this section, we will compare the different numerical methods on a 4D drift-kinetic benchmark, following the paper of *Grangirard et al* [7]. The model is described in section 4.1. We will compute the growth of a 4D unstable turbulent mode. The benchmark consists of exciting the plasma at a single mode (m, n), with m the poloidal mode (θ) and n the toroidal mode (z). The initial distribution function is the sum of an equilibrium and a perturbation distribution function $f = f_{eq} + \delta f$. The equilibrium distribution function has the following form:

$$f_{eq}(r, v_\parallel) = \frac{n_0(r)}{(2\pi T_i(r)/m_i)^{1/2}} \exp\left(-\frac{m_i v_\parallel^2}{2T_i(r)}\right) \tag{79}$$

and the perturbation δf

$$\delta f(r, \theta, z, v_\parallel) = f_{eq}(r, v_\parallel)\ g(r)\ h(v_\parallel)\ \delta p(\theta, z) \tag{80}$$

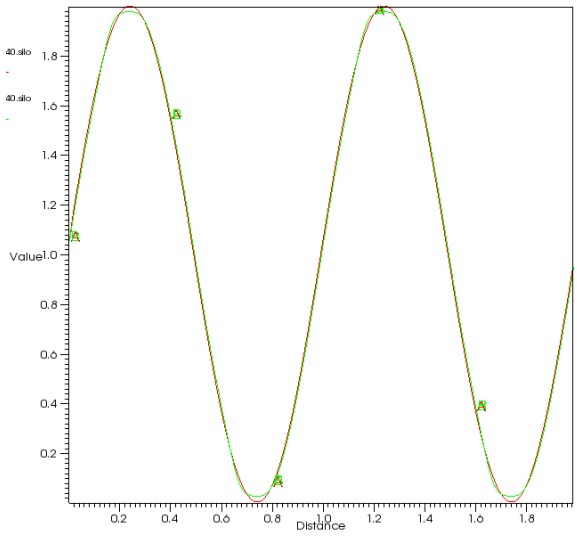

Figure 3: The sinusoidal shape travels 10 times the domain. Domain length 2 with 120 cells. In red without limiter, in green with limiter.

The effect of the limiter is very weak on this benchmark, the curves are almost the same.

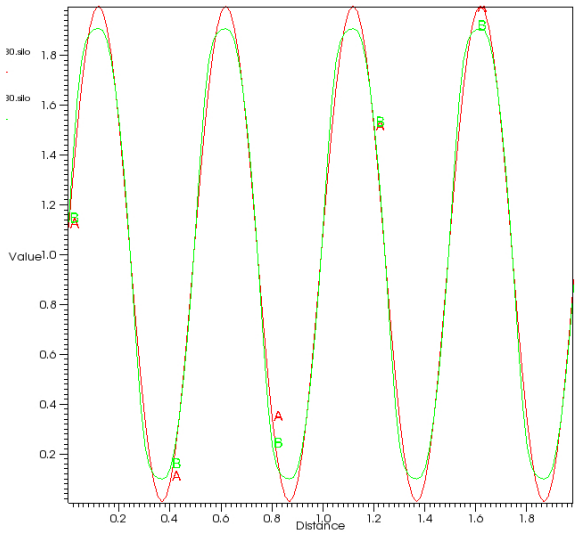

Figure 4: The sinusoidal shape travels 10 times the domain. Domain length 2 with 120 cells. In red without limiter, in green with limiter.

The limiter has two effects when dealing with a steeper function: first it reduces the maxima because of numerical dissipation and second it introduces a slight asymmetry of the function.

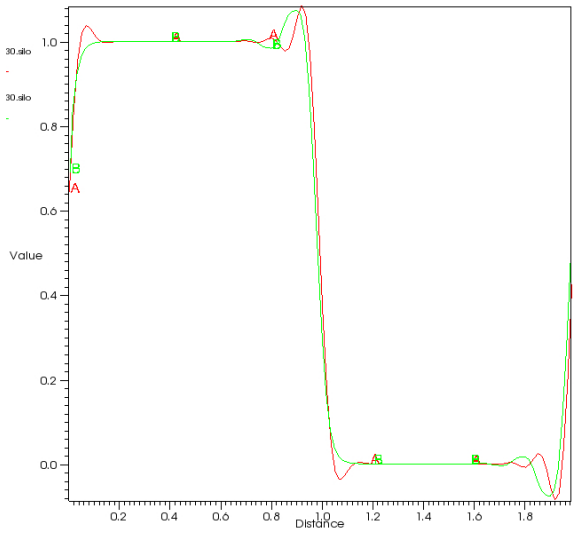

Figure 5: The step shape travels 10 times the domain. Domain length 2 with 120 cells. In red without limiter, in green with limiter.

This benchmark has a discontinuous initial function, which is a step function. Since no maximum principle exists for the PSM scheme, over/undershoots are appearing during the simulation. The limiter has two effects : it reduces the maxima because of numerical dissipation and cut off oscillations in front of the discontinuity (the shape is travelling from left to right). This asymmetric behaviour might be related to the centred scheme that is used to evaluate the dissipative behaviour or not of the PSM scheme: oscillations only appear upwind when using the centred scheme. However, the slope of the solution at the discontinuity (at the center of the graph) is almost the same for both methods, which indicates that little diffusion is introduced by the limiter for this benchmark.

with $g(r)$ and $h(v_\parallel)$ two exponential functions and

$$\delta p(\theta, z) = \epsilon \cos\left(\frac{2\pi n}{L_z} z + m\theta\right)$$

with L_z the length of the domain in z direction, m_i, $T_i(r)$, $n_0(r)$ physical constant profiles, see [7] for details. Here we set $m = 16$ and $n = 4$.
We run different tests comparing results obtained with the BSL scheme, the PSM scheme and the PSM scheme with entropic flux limiter described in section 3.2.

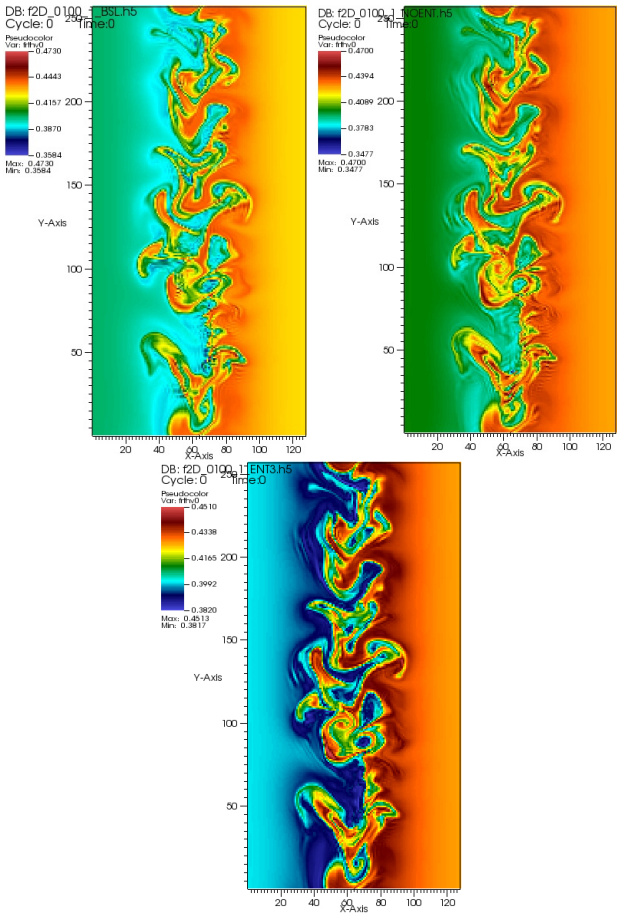

Figure 6: Simulation of 128x256x128x64 cells, comparison BSL (left), PSM (center) and PSM with entropic flux limiter (right), with color scales based on real computed data for each picture rather than set to the same color scale for all of them, time=2000.

These pictures show that the BSL scheme and the PSM scheme do not satisfy a maximum principle, thus "singular" points may appear with values outside initial data bounds, here [0.3873 ; 0.4415]. The PSM scheme with entropic flux limiter has no maximum principle as well, thus "singular" points may appear but the fact that the limiter imposes a diffusive behaviour of the scheme diminishes the spurious extrema.

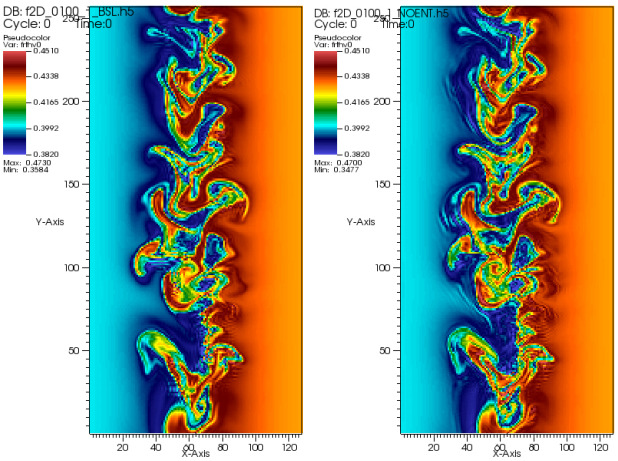

Figure 7: Simulation of 128x256x128x64 cells, comparison BSL (left) and PSM without limiter (right), color scales set to be the same, time=2000.

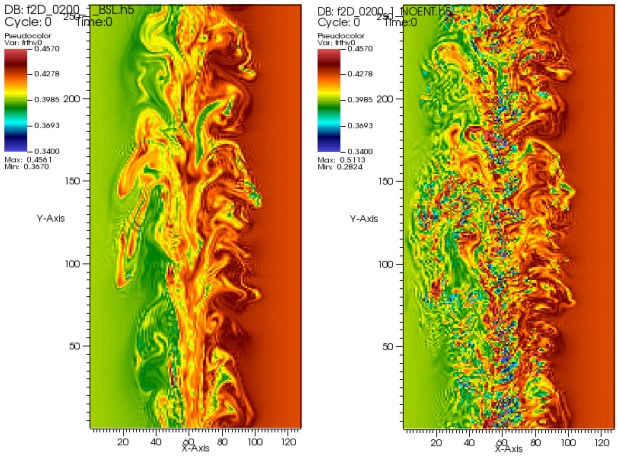

Figure 8: Simulation of 128x256x128x64 cells, comparison BSL (left) and PSM without limiter (right), color scales set to be the same, time =4000.

At time $t = 2000$, BSL and PSM schemes results are very similar. At later time $t = 4000$, the PSM scheme result shows more small structures that are probably mainly spurious oscillations.

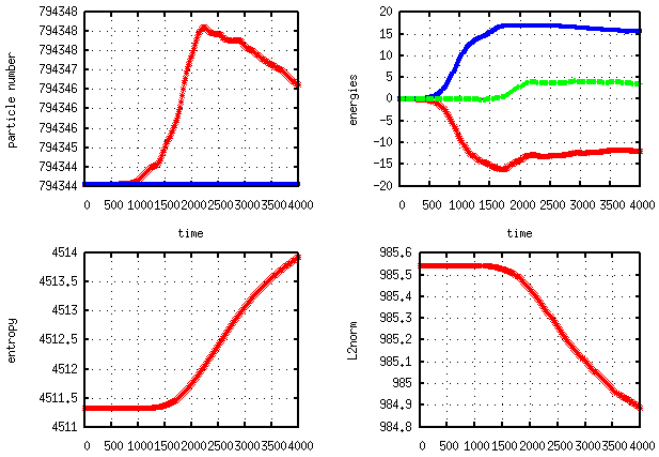

Figure 9: Simulation of 128x256x128x64 cells with BSL scheme.

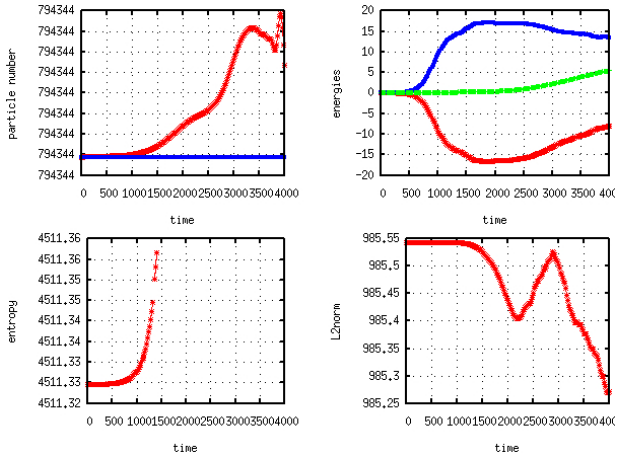

Figure 10: Simulation of 128x256x128x64 cells with PSM scheme.

The particles number (or equivalently the mass) is perfectly kept constant by the PSM scheme. The three curves graph up-right of each picture represents in blue the variation of potential energy, in red the variation of kinetic energy and in green the sum, which corresponds to the variation of total energy that should theoretically be constant to zero. We see in this case that the PSM scheme is a bit better. At bottom right the L^2 norm of the distribution function that should be theoretically kept constant, but decreases with time because of scheme numerical dissipation. We see here a strange behaviour of the PSM scheme, where the L^2 norm increases for a while.

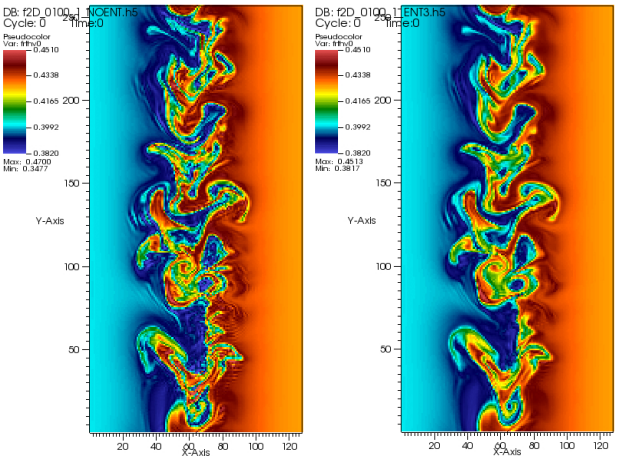

Figure 11: PSM simulation of 128x256x128x64 cells without (left) and with (right) entropic flux limiter, color scales set to be the same, time =2000.

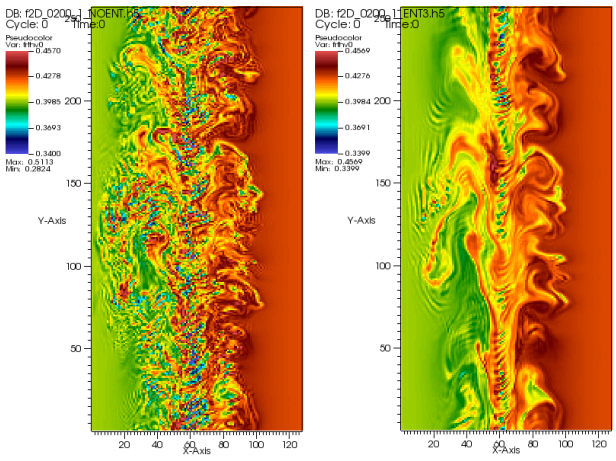

Figure 12: PSM simulation of 128x256x128x64 cells without (left) and with (right) entropic flux limiter, color scales set to be the same, time =4000.

These pictures show that the PSM scheme and the PSM scheme with limiter give qualitatively equivalent results at time $t = 2000$, even if the function is a bit more diffused with limiter. At time $t = 4000$, results are quite different because oscillations are damped by the limiter.

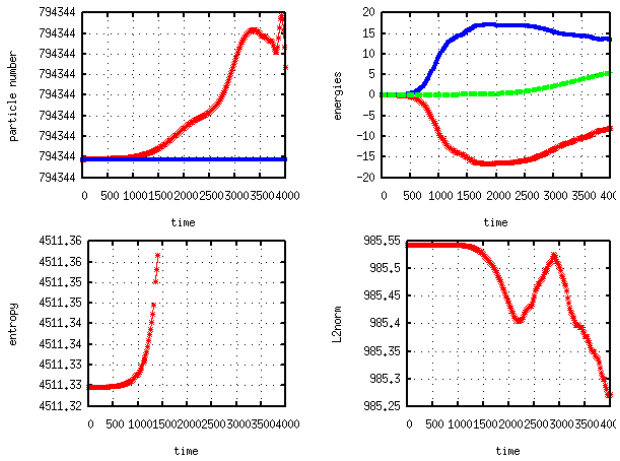

Figure 13: Simulation of 128x256x128x64 cells without entropic flux limiter.

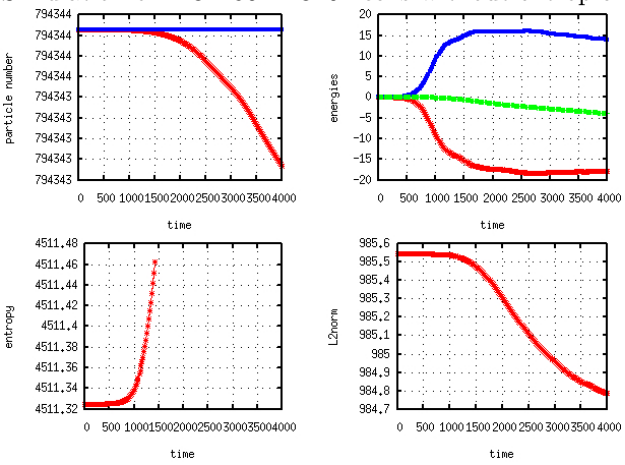

Figure 14: Simulation of 128x256x128x64 cells with entropic flux limiter.

The particles number (or equivalently the mass) is perfectly kept constant by both methods. The three curves graph up-right of each picture represents in blue the variation of potential energy, in red the variation of kinetic energy and in green the sum, which corresponds to the variation of total energy that should theoretically be constant to zero. The PSM scheme with limiter keep the kinetic energy almost constant for large times. At bottom right the L^2 norm of the distribution function that should be theoretically kept constant, but decreases with time because of schemes numerical dissipation. We see that the strange behaviour of the PSM scheme, when the L^2 norm increases for a while, disappears with the limiter.

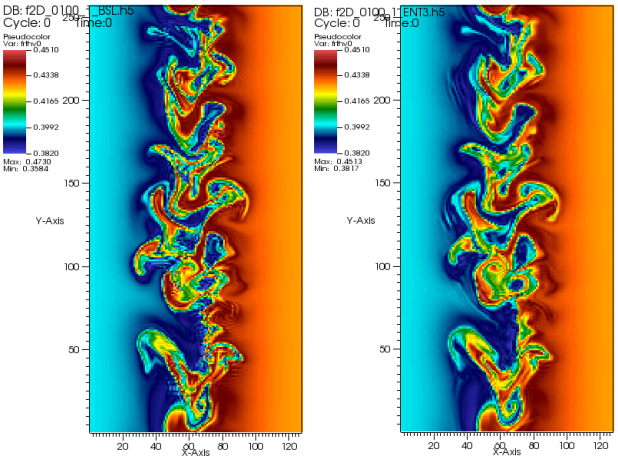

Figure 15: Simulation of 128x256x128x64 cells, comparison BSL (left) and PSM with entropic limiter (right), color scales set to be the same, time=2000.

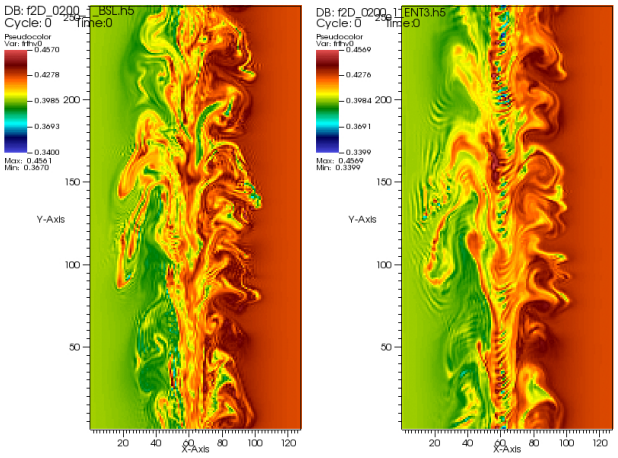

Figure 16: Simulation of 128x256x128x64 cells, comparison BSL (left) and PSM with entropic limiter (right), color scales set to be the same, time =4000.

These pictures show that the BSL scheme and the PSM scheme with limiter give qualitatively equivalent results at time $t = 2000$, even if the function is a bit more diffused for PSM with limiter. At time $t = 4000$, results are similar, but with oscillations at a larger scale for the PSM scheme with limiter than for the BSL scheme. However, the PSM scheme with limiter perfectly conserves the mass and better respects the maximum principle.

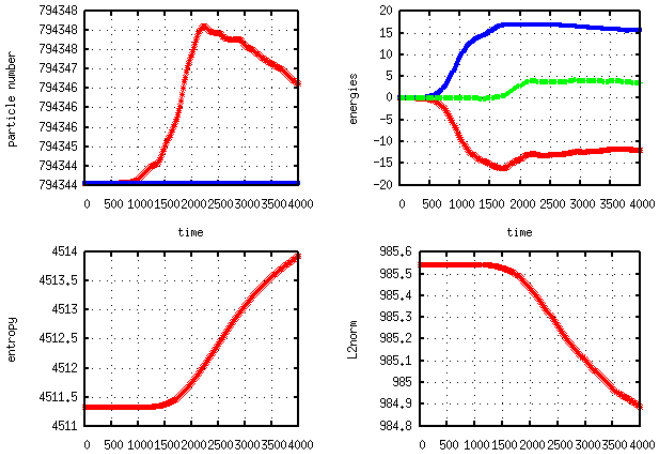

Figure 17: Simulation of 128x256x128x64 cells with BSL scheme.

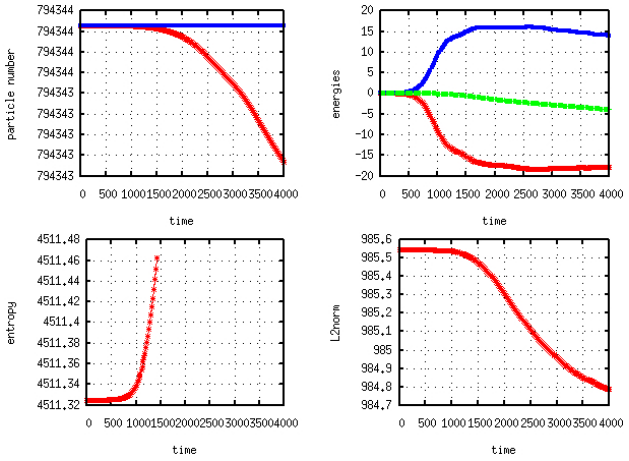

Figure 18: Simulation of 128x256x128x64 cells with PSM scheme with entropic limiter.

The particles number (or equivalently the mass) is perfectly kept constant by the PSM scheme with limiter. The three curves graph up-right of each picture represents in blue the variation of potential energy, in red the variation of kinetic energy and in green the sum, which corresponds to the variation of total energy that should theoretically be constant to zero. The limiter seems to keep the kinetic energy constant. At bottom right the L^2 norm of the distribution function that should be theoretically kept constant, but decreases with time because of schemes numerical dissipation. We see that the BSL scheme and the PSM scheme with limiter give almost the same L^2 norm behaviour.

5 Conclusion

The PSM scheme has been successfully integrated in the GYSELA code and has been tested on 4D benchmarks. We had first experimentally stated and afterward explained in this report that the PSM scheme can be unstable without taking care of a velocity field divergence free condition. Even if a maximum principle has not been strictly proven, the numerical results show that the study of the volume evolution in the phase space is fruitful. Results obtained with the PSM scheme match well qualitatively those obtained with the BSL scheme. Notice that this conservative scheme properly allows a directional splitting when dealing with toroidal geometry, what is not the case with the BSL scheme. The "entropic flux limiter" is efficient to cut off spurious oscillations of the standard PSM scheme and the loss of accuracy seems to be acceptable for these benchmarks. Of course, the PSM scheme should be further validated as well as its integration in the GYSELA code using the gyrokinetic 5D model, that is already functional.

References

[1] A. J. Brizard and T. S. Hahm, Foundations of nonlinear gyrokinetic theory, Rev. Mod. Phys. 79, 421 (2007).

[2] N. Crouseilles, M. Mehrenberger, E. Sonnendrücker, Conservative semi-Lagrangian schemes for Vlasov equations, INRIA Report 6856 (february 2009).

[3] C.Z. Cheng, G. Knorr, The integration of the Vlasov equation in configuration space, J. Comput. Phys. 22, pp. 330-351 (1976).

[4] A. M. Dimits et al, Comparisons and physics basis of tokamak transport models and turbulence simulations, Phys. Plasmas, 7, 969 (2000).

[5] N. Crouseilles, G. Latu, E. Sonnendrücker, A Vlasov solver based on local cubic spline interpolation on patches, J. Comput. Phys., Vol. 228, pp. 1429-1446 (2009).

[6] V. Grandgirard, Y. Sarazin, P. Angelino, A. Bottino, N. Crouseilles, G. Darmet, G. Dif-Pradalier, X. Garbet, Ph. Ghendrih, S. Jolliet, G. Latu, E. Sonnendrücker, L. Villard, Global full-f gyrokinetic simulations of plasma turbulence, Plasma Phys. Control. Fus., Volume 49B, pp. 173–182 (december 2007).

[7] V. Grandgirard, M. Brunetti, P. Bertrand, N. Besse, X. Garbet, P. Ghendrih, G. Manfredi, Y. Sarazin, O. Sauter, E. Sonnendrücker, J. Vaclavik, L. Villard, A drift-kinetic Semi-Lagrangian 4D code for ion turbulence simulation, J. Comput. Physics, vol. 217, no2, pp. 395-423 (2006).

[8] F. Huot, A. Ghizzo, P. Bertrand, E. Sonnendrücker, O. Coulaud, Instability of the time splitting scheme for the one-dimensional and relativistic Vlasov-Maxwell system, J. Comput. Phys., Vol. 185, Issue 2, pp. 512–531 (2003).

[9] R.J. LeVeque, Numerical Methods for Conservation Laws, Birkhäuser (1990).

[10] M. Shoucri, A two-level implicit scheme for the numerical solution of the linearized vorticity equation, Int. J. Numer. Meth. Eng. 17, p. 1525 (1981).

[11] E. Sonnendrücker, J.R. Roche, P. Bertrand, A. Ghizzo, The Semi-Lagrangian Method for the Numerical Resolution of Vlasov Equations, J. Comput. Physics, Vol.149, No.2, pp. 201-220 (1999).

[12] E. Sonnendrücker, Lecture notes CEA-EDF-INRIA, Modèles numériques pour la fusion contrôlée, Nice (Septembre 2008).

[13] M. Zerroukat, N. Wood, A. Staniforth, The parabolic spline method (PSM) for conservative transport problems. Int. J. Numer. Meth. Fluid. v11. 1297-1318 (2006).

[14] M. Zerroukat, N. Wood, A. Staniforth, Application of the parabolic spline method (PSM) to a multi-dimensional conservative semi-Lagrangian transport scheme (SLICE), J. Comput. Phys, Vol. 225 n.1, pp. 935-948 (2007).

Contents

Centre de recherche INRIA Nancy – Grand Est
LORIA, Technopôle de Nancy-Brabois - Campus scientifique
615, rue du Jardin Botanique - BP 101 - 54602 Villers-lès-Nancy Cedex (France)

Centre de recherche INRIA Bordeaux – Sud Ouest : Domaine Universitaire - 351, cours de la Libération - 33405 Talence Cedex
Centre de recherche INRIA Grenoble – Rhône-Alpes : 655, avenue de l'Europe - 38334 Montbonnot Saint-Ismier
Centre de recherche INRIA Lille – Nord Europe : Parc Scientifique de la Haute Borne - 40, avenue Halley - 59650 Villeneuve d'Ascq
Centre de recherche INRIA Paris – Rocquencourt : Domaine de Voluceau - Rocquencourt - BP 105 - 78153 Le Chesnay Cedex
Centre de recherche INRIA Rennes – Bretagne Atlantique : IRISA, Campus universitaire de Beaulieu - 35042 Rennes Cedex
Centre de recherche INRIA Saclay – Île-de-France : Parc Orsay Université - ZAC des Vignes : 4, rue Jacques Monod - 91893 Orsay Cedex
Centre de recherche INRIA Sophia Antipolis – Méditerranée : 2004, route des Lucioles - BP 93 - 06902 Sophia Antipolis Cedex

Éditeur
INRIA - Domaine de Voluceau - Rocquencourt, BP 105 - 78153 Le Chesnay Cedex (France)
http://www.inria.fr
ISSN 0249-6399